

LA-UR- 08-4206

Approved for public release;  
distribution is unlimited.

*Title:* A Multi-Frame, Megahertz CCD Imager

*Author(s):* Jacob A. Mendez  
Stephen J. Balzer  
Scott A. Watson

*Intended for:* IEEE Transactions on Nuclear Science  
SORMA West 2008 Proceedings



Los Alamos National Laboratory, an affirmative action/equal opportunity employer, is operated by the Los Alamos National Security, LLC for the National Nuclear Security Administration of the U.S. Department of Energy under contract DE-AC52-06NA25396. By acceptance of this article, the publisher recognizes that the U.S. Government retains a nonexclusive, royalty-free license to publish or reproduce the published form of this contribution, or to allow others to do so, for U.S. Government purposes. Los Alamos National Laboratory requests that the publisher identify this article as work performed under the auspices of the U.S. Department of Energy. Los Alamos National Laboratory strongly supports academic freedom and a researcher's right to publish; as an institution, however, the Laboratory does not endorse the viewpoint of a publication or guarantee its technical correctness.

# A Multi-Frame, Megahertz CCD Imager

Jacob A. Mendez, *Member IEEE*, Stephen J. Balzer, Scott A. Watson, Robert K. Reich, *Senior Member IEEE*, and Daniel M. O'Mara

**Abstract**—A high-efficiency, high-speed imager has been fabricated capable of framing rates of 2 MHz. This device utilizes a 512 x 512 pixel charge coupled device (CCD) with a 25cm<sup>2</sup> active area, and incorporates an electronic shutter technology designed for back-illuminated CCD's, making this the largest and fastest back-illuminated CCD in the world. Characterizing an imager capable of this frame rate presents unique challenges. High speed LED drivers and intense radioactive sources are needed to perform basic measurements. We investigate properties normally associated with single-frame CCD's such as read noise, gain, full-well capacity, detective quantum efficiency (DQE), sensitivity, and linearity. In addition, we investigate several properties associated with the imager's multi-frame operation such as transient frame response and frame-to-frame isolation while contrasting our measurement techniques and results with more conventional devices.

**Index Terms**—electronically shuttered charge coupled devices, sub-sixel, super-pixel.

## I. INTRODUCTION

RECENTLY the Advanced Imaging Group at the Massachusetts Institute of Technology's Lincoln Laboratory has made advances in buried channel multi-frame CCD arrays capable of frame rates greater than 1MFPS [1]. The device exhibits 100% fill factor and up to four frames can be captured and stored locally in 96 x 96  $\mu\text{m}$  super-pixels. Each super pixel contains 8 (12 x 96  $\mu\text{m}$ ) sub-pixels. There are two sub-pixels per image frame. Figure 1 illustrates

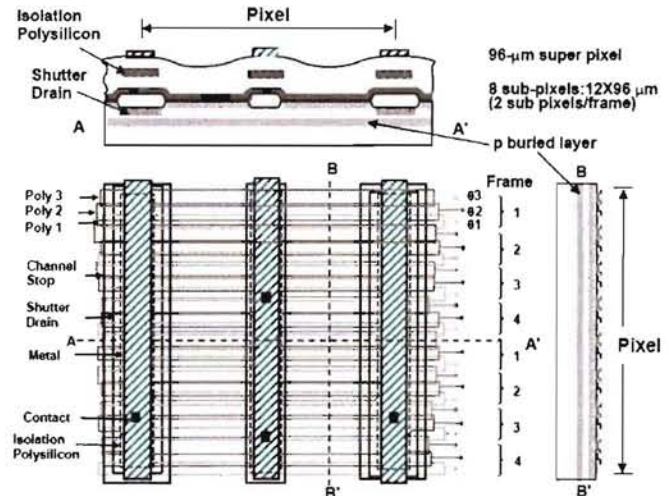


Fig. 1. Top and cross-sectional views of the CCID 36 "super-pixel" structure, note the buried p-layer and the redundant sub-pixel locations A and A'.

the architecture of a super-pixel.

The CCID 36 is a three phase device which employs two phases as electronic shutters during frame integration. To achieve 100% fill factor the super pixel contains two sub-pixels per frame making the collection area of any given frame roughly 96 $\mu\text{m}$  square. The device requires separate current drivers for phases 1 and 2 which correspond to each set of sub-pixels. This allows shuttering of each frame independently at sub-microsecond inter-frame times. In a typical frame sequence phases 1 and 2 of the active frame sub pixels are set to a high voltage typically (15-21V) while phase 3 is held at a low voltage (-6-0V). At these levels phase 1 and 2 collect charge and phase 3 isolates super pixels and sub-pixels. Figure 2 illustrates the shutter open and closed states in an image capture sequence.

The buried channel electronic shutter has been demonstrated with good results for small devices [2]. Employing this technology on larger devices proved difficult due to increased capacitance and relatively high resistivity of the polysilicon gate electrodes. This paper will focus on the device developed jointly by LANL and MIT-LL for use on the DARHT second axis multi-pulse radiographic facility [3].

The high-speed operation of the CCID 36, in excess of 2MFPS, presents unique characterization challenges. In most cases fast light sources and intense radioactive isotopes are required. We discuss the measurement techniques in detail.

Manuscript received June 30, 2008. This work was supported by the U.S. Department of Energy's National Nuclear Security Administration (NNSA) under Contract DE-AC52-06NA25396.

J. A. Mendez is with the Los Alamos National Laboratory, Los Alamos, NM 87545 USA (phone: 505-667-5426; fax: 505-665-3359; e-mail: jmendez@lanl.gov).

S. J. Balzer, is with the Los Alamos National Laboratory, Los Alamos, NM 87545 USA.

S. A. Watson is with the Los Alamos National Laboratory, Los Alamos, NM 87545 USA.

R. K. Reich is with the Lincoln Laboratory, Massachusetts Institute of Technology, Lexington, MA, 02173-9108 USA.

D.M. O'Mara is with the Lincoln Laboratory, Massachusetts Institute of Technology, Lexington, MA, 02173-9108 USA.

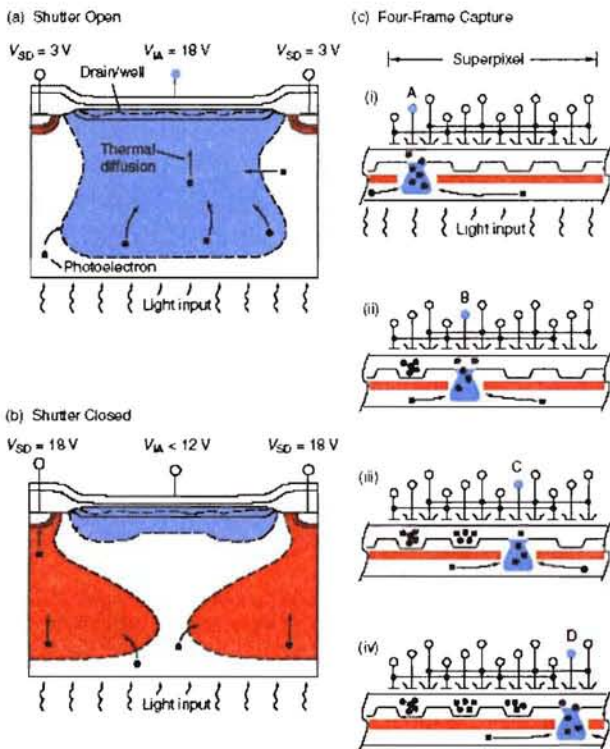


Fig. 2. Top and cross-sectional views of the CCID 36 "super-pixel" structure, note the buried p-layer and the redundant sub-pixel locations A and A'.

## II. PHOTON TRANSFER

The photon transfer technique is used to measure performance characteristics of charge coupled devices [4]. The photon transfer curve (PTC) describes the behavior of the device from noise floor to saturation. Three distinct regions of the curve are illustrated in figure 3 for an ideal detector and three commonly used imaging systems.

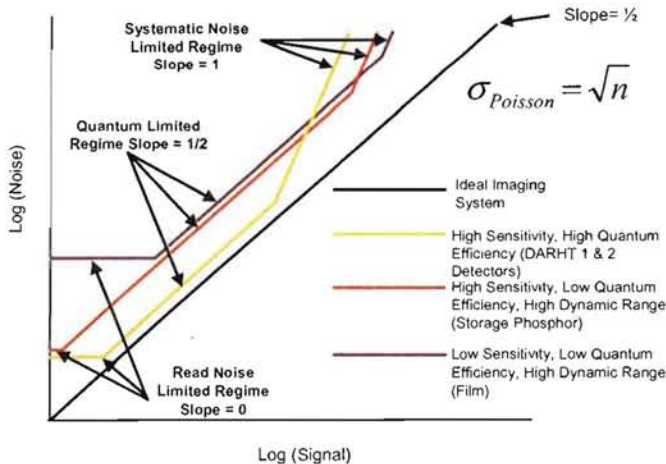


Fig. 3. This graphic of photon transfer curve illustrates three distinct regimes of the curve; 1. Read Noise Limited, 2 Quantum Limited and 3. Systematic Noise Limited, of an ideal imaging system and three commonly used imaging systems. Note the effect of quantum efficiency shown by the distance of the quantum limited regime of an actual imaging system from the counter part region of the ideal imaging system.

TABLE I  
PHOTON TRANSFER RESULTS

Parameter	Measured Value
Gain (electron/count)	4.5
Read Noise (electrons)	10
Full Well (electrons)	120,000

A 420nm LED, driven by an Elantec EL7182C high-speed CCD driver circuit, was used to generate a photon transfer curve. To compensate for the short integration time, the light source is lens coupled to the device. The LED intensity is consistent for a given pulse width but varies with increasing pulse widths up to ~30ns. To eliminate these variations, a fixed pulse width is used and the signal is attenuated using calibrated neutral density (ND) filters. The ND filters range from 0.1 to 3.2 ND and are increased in 0.1 ND increments. Data is collected starting at saturation of the device and reduced by stacking ND filters until the noise floor is reached. The result is a photon transfer curve with an integration time of less than 3  $\mu$ s with over four orders of dynamic range. The photon transfer curve of CCID 36 L6W9C2 is shown in figure 4. Results of the experiment are illustrated in table I.

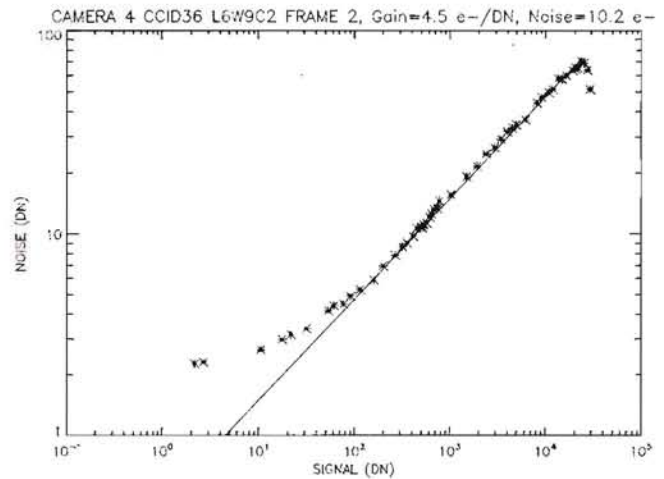


Fig. 4. Photon transfer curve of the CCID 36. The read noise level can be seen in the first data point on the left. Systematic noise is removed by image processing leaving only the quantum limited regime which has a slope of  $1/2$ . Full well is seen at the top of the curve and is identified by the sudden drop in noise while signal continues to increase.

## III. TRANSIENT RESPONSE

Operation at high speeds (>2MHz) requires the use of high-current (>5A), high-speed drivers to operate the CCD shutter phases. The transient response of the imager is measured using a 420nm LED array and reducing optics. A constant 40 ns LED pulse is imaged in 40 ns time increments through the entire frame sequence. The transient response of L6W9C2 is shown in figure 5.

Similar devices developed by MIT-LL have exhibited frame isolation ratios as high as 5,500:1 [2]. The physical size of the CCID 36 ( $25 \text{ cm}^2$ ) leads to limitations in frame isolation performance due to increased device capacitance, resistance

and the number of pixel transfer. Non-Ideal frame isolation causes “ghosting,” or charge sharing between frames, an example of this is seen in figure 6. New process methods are currently being implemented in Lot 6b CCID 36 devices to improve frame isolation.

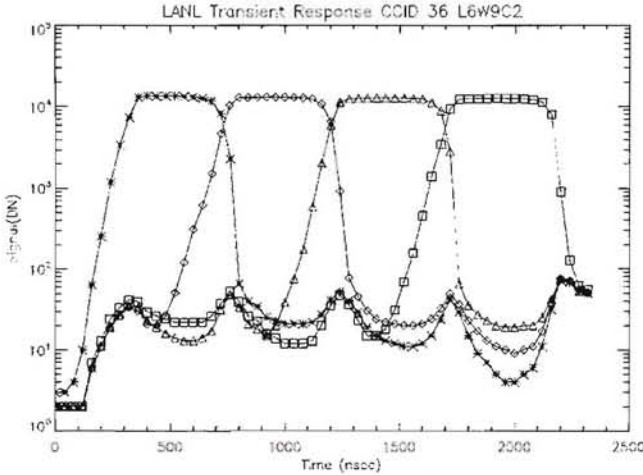


Fig. 5. Transient frame response illustrating a four frame capture at 2MFPS.

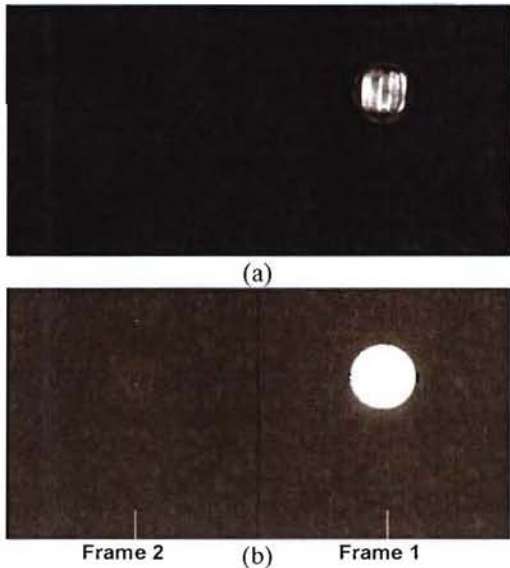


Fig. 6. Image sets (a) and (b) are the same image displayed at different thresholds. Image set (a) shows the full scale image while a threshold is applied to reveal “ghosting” in image set (b).

The frame isolation is measured as a ratio of two frames and is calculated directly from the transient frame response. The isolation ratio is influenced by variables such as charge transfer efficiency, ion implantation (p+ buried channel) and substrate thickness. The isolation measured for this device exceeded 500:1. Improvements in process methods and design are currently underway to increase the ratio to >1000:1.

#### IV. LINEARITY

Linearity was measured using an LED, driven by a high-

speed pulse circuit. To eliminate variations in light output, the data is fit to an equation describing the LED output characteristics. The LED transfer curve is shown in figure 5. Using this method a linearity of 9% (maximum deviation over 12 bits) is measured. A fractional non-linearity residual curve over the entire dynamic range is shown in figure 7.

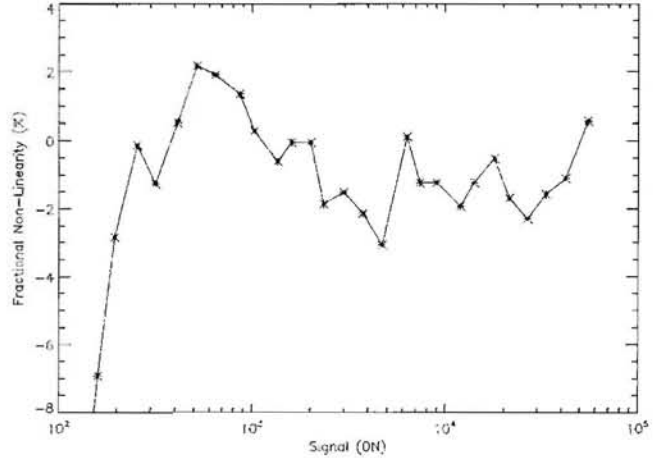


Fig. 7. Linearity residual curve showing fractional non-linearity of +/-3% maximum deviation over 12 bits.

#### V. DETECTIVE QUANTUM EFFICIENCY

The detective quantum efficiency (DQE) is a metric used to describe the statistical noise performance of imaging systems [5].

The *DQE* can be computed from

$$DQE(f) = \frac{MTF^2(f)}{NPS(f)NEQ(f)}, \quad (1)$$

where  $DQE(f)$  is the detective quantum efficiency,  $MTF(f)$  is the modulation transfer function value at spatial frequency  $f$  (cycles/mm),  $NPS(f)$  is the noise power spectrum value ( $1/\text{mm}^2$ ) at spatial frequency  $f$  (cycles/mm), and  $NEQ$  is the noise equivalent quanta generated at a given exposure.

A modified version of the detector blur first proposed by Swank [6] is used for the detector MTF and is given by

$$MTF_{\text{Detector}}(f) = \frac{1}{1 + \left(\frac{f}{mf_c}\right)^2}, \quad (2)$$

where  $f_c$  is the detector cutoff frequency (cycles/mm).

For a mono-energetic source,  $NEQ(f)$  is proportional to the NIST source activity (16.6 x-ray photons/ $\mu\text{R}$  for  $\text{Co}^{60}$ ) [7].

The  $NPS(f)$  was calculated from the difference of two 340  $\mu\text{R}$  exposures and as such the difference image systematic errors cancel out while its variance doubles. Hence, the  $NPS$  obtained is similar to that obtained from a half value or 170  $\pm$  5  $\mu\text{R}$  exposure yielding an  $NEQ$  of 2,800  $\pm$  100 x-ray photons. The  $NPS$  numerical estimation was obtained using

the method of Hanson [8] and is shown in figure 8.

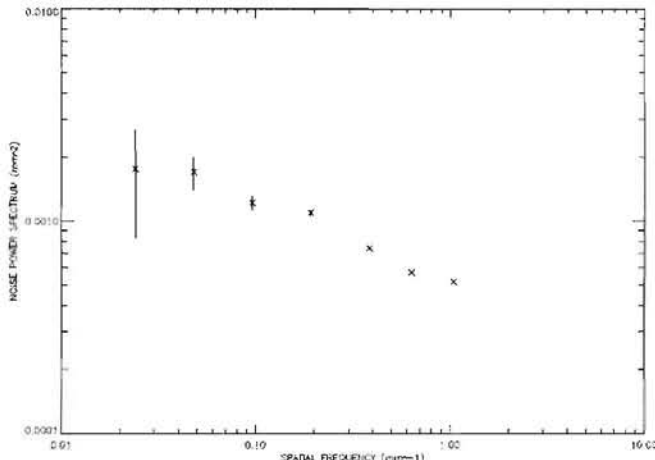


Fig. 8. Noise power spectrum with a 170  $\mu\text{R}$  exposure using a NIST traceable  $\text{Co}^{60}$  source and LSO scintillator.

A NIST traceable, 1 mm diameter,  $35.5 \pm 0.1$  Gbq, 1.25 MeV,  $\text{Co}^{60}$  source is used. This source was chosen because of the difficulty obtaining a calibrated, low-dose, megavolt Bremmstrahlung source [9]. The source is used to activate an 45 cm diameter, 1.1 mm pixel pitch, 4 cm-thick Cesium-doped Lutetium Oxyorthosilicate  $\text{Lu}_2\text{SiO}_5:\text{Ce}$  (LSO) segmented scintillator [10]. Light emitted from the scintillator is directed to the CCID36 by a 45 degree turning mirror. A double Gauss F1.5 lens assembly is used to focus the image onto the CCD face. The lens-coupled system has a focal length of 950 mm from the surface of the scintillator to the surface of the first lens element. Figure 7 shows the experimental setup for performing the measurement.

The two 340  $\mu\text{R}$  exposures were obtained by placing the source 69 cm from the surface of the scintillator array during a 4 frame, 400 ms exposure. The CCID36 shutter drain prevents any residual charge from being collected during the manual exposure (3-4 sec.). The shutter drain is taken to a +15V after the four frames are integrated, thereby removing any charge generated after the 400ms exposure. Several images were taken, to quantify the effect of exposure time of the source with respect to the exposure time of the imager. No detrimental effects were seen. A bias image was taken for each image to remove the bias signal from the  $\text{Co}^{60}$  exposures. The measured gamma ray  $DQE(0.023)$  of the CCID 36 using LSO is  $0.45 \pm 0.10$ .

## VI. SENSITIVITY

With a known source activity, the sensitivity of a CCD imager can be determined through histogram analysis of an exposure image. The main event peak in the histogram is a digital representation of the radiation source to charge signature. This peak can be directly related to the source activity  $R$ , in Roentgens per hour (R/hr). The sensitivity is the ratio of the histogram peak  $S(DN)$  to the source exposure  $R$  given by

$$S_{\text{CCD}} = \frac{S(DN)}{R}. \quad (3)$$

The source exposure  $R$  is calculated from the source activity given by

$$R = \frac{GE(f)}{6r^2}, \quad (4)$$

where  $R$  is the exposure rate (Roentgens/hour) at a distance  $r$ ,  $E$  is the total photon energy (MeV),  $G$  is the source activity in (GBq),  $f$  is the decimal fraction of photon yield, 6 is a conversion constant and  $r$  is the distance from the point source (ft.) [11].

The measured sensitivity using (3) with LSO is 5.9 DN/ $\mu\text{R}$ .

Using the read noise of the imager, 1.5 DN, and the result from (3) the Noise Equivalent Sensitivity (NES) can be calculated. The NES of the CCID 36, using LSO, is 0.2  $\mu\text{R}$ .

## VII. CONCLUSION

With the advances in electronically shuttered CCD's many difficult experiments are now realizable. Applying advanced semiconductor manufacturing techniques, a fast imager >1MFS, the CCID 36 provides sensitivity comparable to the devices on the Hubble telescope with the photographic speed of a rotating mirror framing camera.

## REFERENCES

- [1] R. K. Reich, "Integrated Electronic Shutter for Back-Illuminated Charge-Coupled Devices," *IEEE Trans. Electron Devices*, vol. ED-40, no. 7 pp. 1231-1237, July. 1993.
- [2] R. K. Reich, "Sub-Poisson Statistics Observed in an Electronically Shuttered and Back-Illuminated CCD Pixel," *IEEE Trans. Electron Devices*, vol. ED-44, no. 1 pp. 69-73, January. 1997.
- [3] B. T. McCustian, "DARHT-II Commissioning Status," Pulsed Power Conference 14<sup>th</sup> International IEEE digest of technical papers, vol. 1 pp. 391-394, June. 2003.
- [4] J. R. Janesick, *Scientific Charge-Coupled Devices*. Washington: SPIE Press, 2000, ch. 2.
- [5] I. A. Cunningham, "Signal-to-Noise optimization of medical imaging systems," *J. Opt. Soc. Amer.*, vol. 16, no. 3 pp. 621-632, March. 1999.
- [6] R. K. Swank, "Calculation of Modulation Transfer Functions of x-ray Fluorescent Screens," *Appl. Opt.*, vol. ED-12, no. 8 pp. 1865-1870, August. 1973.
- [7] E. H. Johns, *The Physics of Radiology*. Illinois: Charles C. Thomas Pub., 1983.
- [8] K. M. Hanson, "A Simplified Method of Estimating Noise Power Spectra," *Phys. Med. Img.*, vol. 3336, pp. 243-250. 1998.
- [9] S. A. Watson, "Quantum Efficiency, noise Power Spectrum, Linearity and Sensitivity of the DARHT  $\gamma$ -Ray Camera," Los Alamos National Lab., Los Alamos, NM Rep. LA-UR-95-3570, 1995.
- [10] S. A. Watson, "The DARHT Camera," Los Alamos National Lab., Los Alamos, NM Los Alamos Science Magazine, pp. 92-95, 2003.
- [11] M. W. Lantz, "Using the 6CE Rule With SI Units," RSO Magazine, Z-RSO-5028, vol. 2, pp. 12-15. February. 1997.